CHEMISTRY OF MATERIALS

pubs.acs.org/cm

Article

One-Dimensional Organic–Metal Halide with Highly Efficient Warm White-Light Emission and Its Moisture-Induced Structural Transformation

Guicheng Yu, Fang Lin, Kang Zhou, Shaofan Fang, Yumeng Shi, Wei Liu, Hanlin Hu, Biwu Ma, and Haoran Lin*

Cite This: *Chem. Mater.* 2021, 33, 5668–5674

Read Online

ACCESS | Metrics & More | Article Recommendations | Supporting Information

ABSTRACT: Molecular low-dimensional organic–metal halide hybrids have shown great potentials as light emitters with excellent color tunability. High photoluminescence quantum efficiency (PLQE) and high color rendering index (CRI) are two essential requirements for them to act as down conversion phosphors to achieve single-component white-light emission. Here, we report an organic–metal halide hybrid $[C_4N_2H_{12}]_3[PbBr_5]_2{\cdot}4DMSO$ with a one-dimensional (1D) structure at the molecular level, which possesses a record-setting PLQE of 60% and high CRI value of 84 as a promising single-component white-light emitter. We have also experimentally observed the photoluminescence quenching of $[C_4N_2H_{12}]_3[PbBr_5]_2{\cdot}4DMSO$ and its transformation to 0D $[C_4N_2H_{12}]_4[Pb_2Br_{11}]Br{\cdot}4H_2O$, which suggests that the degradation process involves water-molecule replacement and moisture-induced cleavage of 1D lead halide chains.

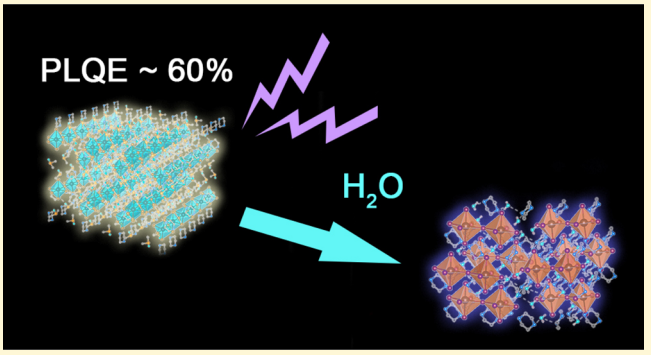

INTRODUCTION

Metal halide perovskites and perovskite-related materials have become a rising star during the last decade with extensive applications in a wide range of areas, including photovoltaics, light-emitting diodes (LEDs), lasers, scintillators, and so forth.[1−3] Low-dimensional metal halide hybrids, benefitting from their high exciton binding energies and efficient radiative recombination, are intensely studied as promising light emitting materials in recent years.[4,5] Among the low-dimensional metal halide hybrid family, organic–metal halide hybrids with a one-dimensional (1D) structure at the molecular level are single crystals consisting of bundles of ionic metal halide wires/chains/tubes surrounded and separated by organic cations. Researchers have reported some examples of 1D organic–metal halide hybrids in past few years.[6] For example, the pioneer work of Yuan *et al.* reported a 1D organic–metal halide exhibiting bluish white-light emission with a photoluminescent quantum efficiency (PLQE) of 20%.[7] Another 1D material PzPbBr, with bulk assembly of contorted lead halide chains, was reported by Biswas and his colleagues to exhibit yellowish-white light and a PLQE of ~9%.[8] Gautier *et al.* recently developed a 1D lead halide postperovskite-type material $(TDMP)PbBr_4$, which possesses a PLQE of 45%, the highest PLQE at room temperature and ambient pressure reported to date, and a color rendering index (CRI) of 75.[9] The commonly observed broad-band emissions in these materials suggest that they could act as single-component white-light emitters for various applications. Great efforts have been made to further develop new 1D organic–metal halide materials including those using nonlead elements and to investigate their structural–property relationships.[10−18] Recent research studies also discovered that the PLQE of the 1D organic–metal halide compounds could be greatly enhanced under high pressure due to effective tuning of self-trapped states and suppression of nonradiative decay.[19−21] However, the PLQE and CRI values of these reported 1D metal halides are still not ideal, and their degradation mechanisms under ambient conditions have not been well studied yet.[22]

Here, we report the synthesis and photoluminescence (PL) properties of a novel molecular 1D organic–metal halide hybrid $[C_4N_2H_{12}]_3[PbBr_5]_2{\cdot}4DMSO$, which structurally represents 1D corner-sharing chains derived from conventional three-dimensional (3D) lead halide perovskites. Yellowish-white-light emission is observed from this hybrid material with an unprecedented PLQE of around 60% and a high CRI of 84. Interestingly, this 1D organic–metal halide hybrid went

Received: April 8, 2021
Revised: June 30, 2021
Published: July 13, 2021

https://doi.org/10.1021/acs.chemmater.1c01219
Chem. Mater. 2021, 33, 5668–5674

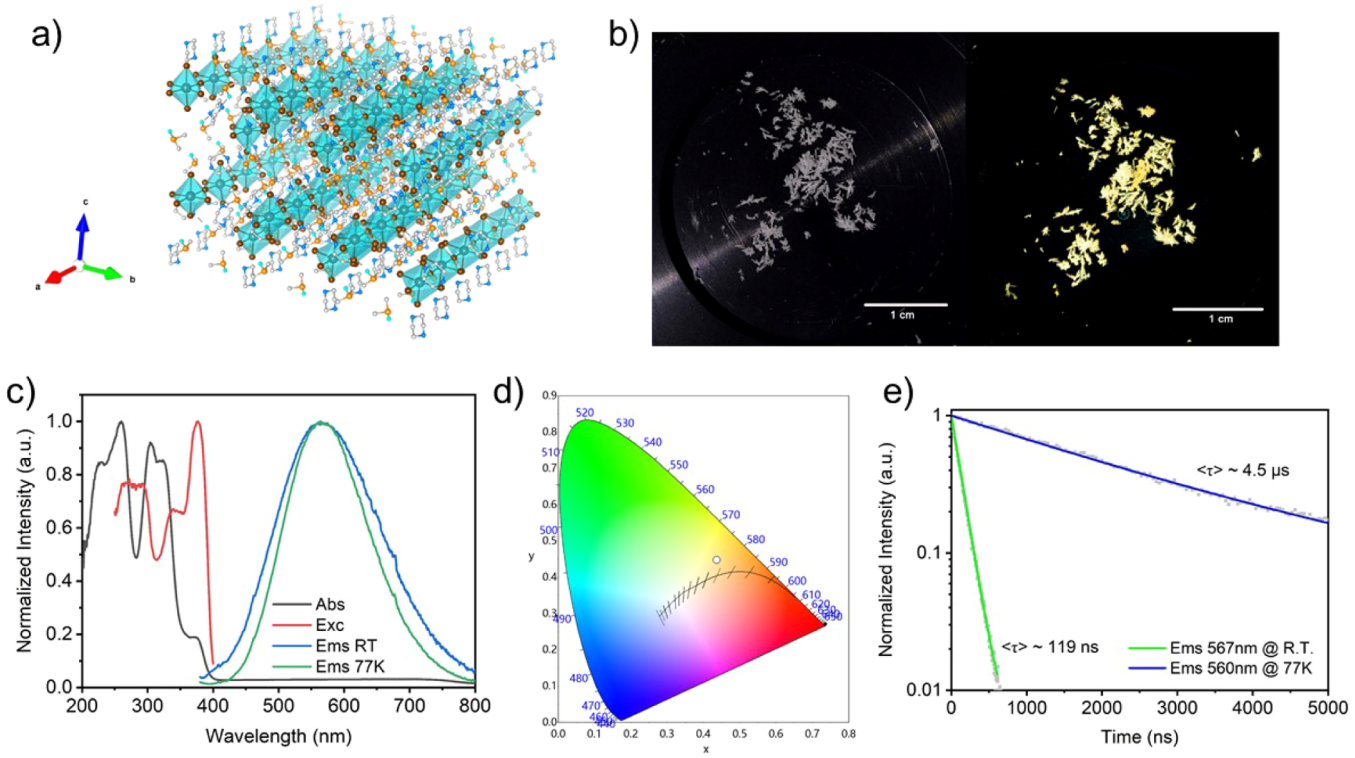

Figure 1. (a) Crystal structure of 1D $[C_4N_2H_{12}]_3[PbBr_5]_2$·4DMSO containing corner-shared metal halide octahedra chains. (b) Photograph of $[C_4N_2H_{12}]_3[PbBr_5]_2$·4DMSO crystals under ambient (left) and 370 nm UV light (right). (c) Optical properties (absorption, excitation, and emission spectra) of $[C_4N_2H_{12}]_3[PbBr_5]_2$·4DMSO crystals. (d) CIE 1933 chromaticity coordinates of the $[C_4N_2H_{12}]_3[PbBr_5]_2$·4DMSO crystals. The CCT and CRI are calculated to be 3336 K and 84, respectively. Data collected under a 370 nm monochrome lamp at R.T. (e) PL decay curves and exponential fitting of the curves of the $[C_4N_2H_{12}]_3[PbBr_5]_2$·4DMSO crystals at room temperature (blue line) and 77 K (green line). Data collected under excitation of a 365 nm monochromatic LED laser.

through a PL quenching when stored in air and gradually turned into a new zero-dimensional (0D) compound $[C_4N_2H_{12}]_4[Pb_2Br_{11}]Br·4H_2O$. Further characterizations suggest that the degradation process involves the intercalation of H_2O and cleavage of the 1D metal halide chains. The high PLQE and CRI values of $[C_4N_2H_{12}]_3[PbBr_5]_2$·4DMSO indicate its potential applications in solid-state lighting and optical moisture sensors.

EXPERIMENTAL RESULTS

Single crystals of $[C_4N_2H_{12}]_3[PbBr_5]_2$·4DMSO can be prepared by slowly diffusing dichloromethane (DCM) into a solution of pyrazine dihydrobromide ($C_4N_2H_{12}Br_2$) and $PbBr_2$ in a mixed solvent of dimethylformamide (DMF) and dimethylsulfoxide (DMSO). (Synthesis details are given in Supporting Information). Single-crystal X-ray diffraction (SCXRD) was applied for the structure determination. The results revealed that the single crystal of $[C_4N_2H_{12}]_3[PbBr_5]_2$·4DMSO has a monoclinic space group $P2_1/c$, and the relevant crystallographic details are summarized in Tables S1, S2. The crystal structure was validated by the similar experimental and simulated powder X-ray diffraction (PXRD) spectra (Figure S1). In the single crystal, $PbBr_6$ octahedra were linked with each other through corner sharing, forming 1D lead bromide straight chains. Three $[C_4N_2H_{12}]^{2+}$ cations and four solvent DMSO molecules sat around the 1D $[PbBr_5]_\infty$ chain in the monoclinic unit cell, isolating them from each other. Also, N−H···O hydrogen bonds were found between the ammonium groups from $[C_4N_2H_{12}]^{2+}$ cations and the O atoms in DMSO, which might promote photoemission.[23] $[C_4N_2H_{12}]_3[PbBr_5]_2$·4DMSO could be regarded as a bulk assembly of 1D perovskite-type chains, with the same structural terminology derived from the 3D metal halide perovskite (Figure 1a). Figure S2 presents different angle views of the crystal structure along *a*, *b*, and *c* axes of this 1D organic−metal halide hybrid. The $PbBr_6$ units in the 1D chains deviate from perfect octahedron, resulting in tilting of the 1D chains and two crystallographically inequivalent Pb octahedra.

We characterized the photophysical properties of $[C_4N_2H_{12}]_3[PbBr_5]_2$·4DMSO under different conditions. The crystals are colorless needles under ambient light and exhibit warm white-light emission when irradiated by a 370 nm ultraviolet−visible (UV) lamp (Figure 1b). The absorption, excitation, and emission spectra of $[C_4N_2H_{12}]_3[PbBr_5]_2$·4DMSO at room temperature are shown in Figure 1c. The absorption onset is at 390 nm, indicating an optical band gap of 3.18 eV. The excitation spectrum matches well with the absorbance, exhibiting two main excitation peaks at 280 and 372 nm. The emission spectrum is almost excitation-independent (Figure S3). When excited by 370 nm monochromatic light, $[C_4N_2H_{12}]_3[PbBr_5]_2$·4DMSO exhibited a broad-band PL emission that covers almost the entire visible-light region, with the peak value at around 560 nm.

Under such conditions, the Commission Internationale de l'Eclairage (CIE) coordinates and the correlated color temperature (CCT) of the yellowish-white-light emission was determined to be (0.4361, 0.4474) and 3336 K, respectively (Figure 1d). The CRI value reaches 84 under ambient conditions, which are comparable to the recommended value for commercialized LEDs (approximately 80). Also, $[C_4N_2H_{12}]_3[PbBr_5]_2$·4DMSO achieved a PLQE of 60% under 335 nm excitation (Figure S4), which is an outstandingly high PLQE value among 1D organic−lead halide hybrids. While excited by 370 nm UV light at 77 K, the PL emission of this 1D material became narrower with an almost unchanged peak value.

Time-resolved photoluminescence spectra of the PL peaks are shown in Figure 1e. The lifetimes of the peaks were calculated to be 119 ns at room temperature and 4.5 μs at 77 K using biexponential fitting (detailed fitting formulas are listed in the Supporting Information).

https://doi.org/10.1021/acs.chemmater.1c01219
Chem. Mater. 2021, 33, 5668−5674

Table 1. Comparison of Crystal Parameters of the 1D Organic−Metal Halide Hybrids

compound	PLQY[%]	λ_{oct}	$\sigma^2_{oct}[^{o2}]$	D	ref
PzPbBr-Pb1	9	1.000771	16.84	0.7512	8
PzPbBr-Pb2	9	1.000791	17.12	0.6612	8
$(C_4N_2H_{14})PbCl_4$	18	1.005000	8.28	0.7477	27
$[C_4N_2H_{12}]_3[PbBr_5]_2$·4DMSO-Pb1	60	1.000439	22.83	0.4459	this work
$[C_4N_2H_{12}]_3[PbBr_5]_2$·4DMSO-Pb2	60	1.000433	17.99	0.4417	this work

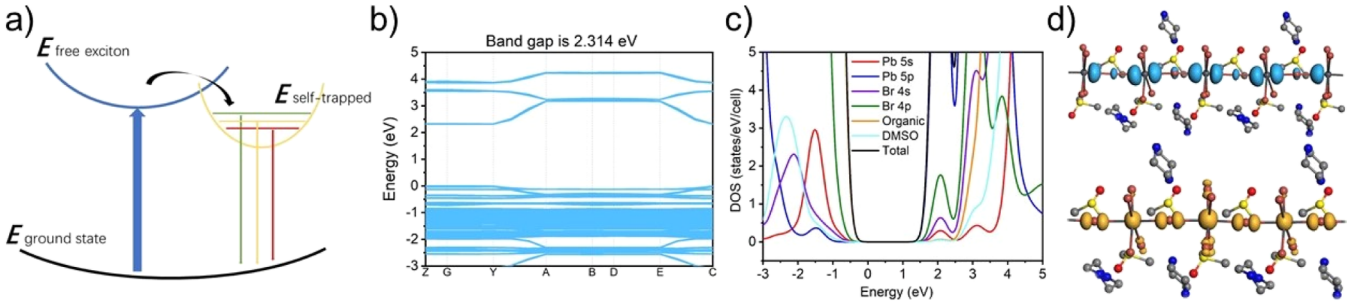

Figure 2. (a) Self-trapped emission mechanism for $[C_4N_2H_{12}]_3[PbBr_5]_2$·4DMSO crystals. (b) Calculated band structure of 1D $[C_4N_2H_{12}]_3[PbBr_5]_2$·4DMSO. (c) Density of states of 1D $[C_4N_2H_{12}]_3[PbBr_5]_2$·4DMSO. (d) Spatial contour plots of antibonding (upper) and bonding frontier orbitals (below).

Table 2. Comparison of Lifetime Values of the Lead Halide Materials

material	PLQY[%]	Ave τ[ns]	Ave τ_r[ns]	Ave τ_{nr}[ns]	Ref.
PzPbBr	9	39.6	440.0	43.5	8
$(C_4N_2H_{14})PbCl_4$	18	20.0	111.1	24.4	27
$[C_4N_2H_{12}]_3[PbBr_5]_2$·4DMSO	59	119.0	203.0	288.0	This work

The structural distortion of the lead halide octahedra in the 1D organic−metal halides is believed to be a critical factor affecting their optical properties. The degree of structural distortion can be described by octahedral elongation λ_{oct}, as well as octahedral angle variance σ^2_{oct} using the following formulas[24]

$$\lambda oct = \frac{1}{6}\sum_{i=1}^{6}\left(\frac{di}{do}\right)^2$$

$$\sigma^2 oct = \frac{1}{11}\sum_{i=1}^{12}(\alpha i - 90)^2$$

where, d_i are six independent Pb−Br bond lengths, d_0 is the average Pb−Br bond length, and α_i refer to Br−Pb−Br angles. On the basis of the structural parameter in Table S3, the octahedral elongation λ_{oct} for two types of octahedra were calculated to be 1.000439 and 1.000433, and the octahedral angle variances $\sigma_{oct}{}^2$ were separately determined to be 22.83 and 17.99^{o2}. Recently, Lü and his colleagues proposed a novel insight of the structure−property relationship in halide perovskites. They found a quantitative relationship between the D parameter describing the degree of off-centering distortion of the MX_6 (M = Ge, Sn and Pb, X = Cl. Br, I) octahedron and the emission efficiency. The D parameter is expressed as follows[25,26]

$$D = \sum_{i=1}^{3}\frac{|a_i - b_i|}{a_i + b_i}$$

where a_i and b_i refer to the short and long M−X bond distances, respectively, in one direction. The D parameter is determined to be 0.4459 and 0.4417, respectively. We have listed the parameters describing the degree of distortion of the 1D compounds mentioned above in Table 1.[27] By comparing these parameters, we found that the octahedral elongation parameter λ_{oct} and the off-centering distortion parameter D of $[C_4N_2H_{12}]_3[PbBr_5]_2$·4DMSO is the smallest among all three compounds, indicating similar Pb−Br bond lengths. Note that the emission-D relation of our samples matches the principle revealed by Lü *et al.* very well.[25] However, the $\sigma_{oct}{}^2$ of $[C_4N_2H_{12}]_3[PbBr_5]_2$·4DMSO is the largest among the three, suggesting that the distortion of $PbBr_6$ octahedra is mainly attributed to the Br−Pb−Br bond angle deviation. The distortion of $PbBr_6$ octahedra described by the small λ_{oct}, D parameter as well as large $\sigma_{oct}{}^2$ of $[C_4N_2H_{12}]_3[PbBr_5]_2$·4DMSO is a critical factor to achieve its high PLQE.[28]

The large Stokes shift (1.21 eV) of the broad-band emission and its long PL lifetime suggest an excitonic self-trapped emission, which was commonly observed in low-dimensional organic−metal halide systems. Upon excitation, free excitons are first formed due to the large exciton binding energy in 1D organic−metal halide hybrids.[29] Strong exciton−phonon coupling then results in the fast self-trapping and localization of excitons, further reducing the emission energy, as shown in Figure 2a. We also obtained the temperature-dependent PL emission of $[C_4N_2H_{12}]_3[PbBr_5]_2$·4DMSO in the temperature range of 77 K to room temperature (Figure S5). The unchanged peak position indicates similar self-trapped excitonic states under a wide temperature range. Also, the absence of direct band emission indicates a low or no free excitonic states to self-trapped excitonic state energy barrier for excitons to overcome.

To further investigate the origin of the high PLQE, the average PL decay lifetime (τ) together with the PLQE was used to calculate the radiative decay lifetime (τ_r) and nonradiative decay lifetime (τ_{nr}) based on the following equations[30]

$$PLQE = \frac{1}{\tau_r}/\left(\frac{1}{\tau_r} + \frac{1}{\tau_{nr}}\right)$$

$$\frac{1}{\tau} = \frac{1}{\tau_r} + \frac{1}{\tau_{nr}}$$

The calculated τ_r and τ_{nr} for $[C_4N_2H_{12}]_3[PbBr_5]_2$·4DMSO and previously reported ones are listed in Table 2. Although $[C_4N_2H_{12}]_3[PbBr_5]_2$·4DMSO possesses comparable τ_r than τ_r of the other two compounds, its τ_{nr} is far larger than that of the other two.

https://doi.org/10.1021/acs.chemmater.1c01219
Chem. Mater. 2021, 33, 5668−5674

The longest nonradiative lifetime of $[C_4N_2H_{12}]_3[PbBr_5]_2{\cdot}4DMSO$ indicates the slowest nonradiative decay process, which means that the high PLQE of $[C_4N_2H_{12}]_3[PbBr_5]_2{\cdot}4DMSO$ mainly originates from the suppressed nonradiative recombination pathways.

To validate the origin of the self-trapped emission, density functional theory (DFT) calculation based on the pseudopotential plane wave (PPW) method was performed. (Detailed calculation methods are stated in Supporting Information). As shown in Figure 2b, the calculated band gap for 1D $[C_4N_2H_{12}]_3[PbBr_5]_2{\cdot}4DMSO$ is 2.314 eV, which is expected to be underestimated due to the well-known PBE band gap error. The calculated highest occupied molecular orbital (HOMO) is relatively flat, reflecting highly localized electronic states. The projected density of states (DOS) (Figure 2c) shows that the ground states near the band edge mainly consist of organic cations, Br 4p and Pb 5s hybrid orbitals, and the excited states near the band edge are mainly composed of Pb 5p and Br 4p hybrid orbitals. However, the spatial contour plots of bonding and antibonding frontier orbitals of 1D $[C_4N_2H_{12}]_3[PbBr_5]_2{\cdot}4DMSO$ shows negligible contribution of the organic cations (Figure 2d), and the excitons are highly localized within lead bromide octahedra, supporting that the emission indeed comes from the self-trapped excitons on the 1D chains.

To study the potential applications of this 1D perovskite material, we first characterized its stability under ambient conditions. We found that the PL of $[C_4N_2H_{12}]_3[PbBr_5]_2{\cdot}4DMSO$ remained stable under an inert atmosphere but gradually quenched when exposed to air in a time period of 16 h (Figure S6). Many metal halide perovskite materials are reported to lack long-term stability in the presence of light or water,[31] but the degradation mechanism for low-dimensional organic−metal halides are rarely studied. To gain more insights of the degradation process, we first characterized the single-crystal structure of the damp sample and found that a new 0D compound formed with the chemical formula of $[C_4N_2H_{12}]_4[Pb_2Br_{11}]Br{\cdot}4H_2O$. Interestingly, the crystals contain isolated $Pb_2Br_{11}^{7-}$ dimers (Figure 3a). Comprehensive crystallographic data and various angles of views of this 0D organic−lead halide material are provided in Table S4 and Figure S7, which are further confirmed by the PXRD experiment (Figure S8a). This 0D material remains stable under ambient conditions for over 6 months, as proved by the unchanged PXRD patterns (Figure S8b). When comparing the crystal structure of $[C_4N_2H_{12}]_3[PbBr_5]_2{\cdot}4DMSO$ with $[C_4N_2H_{12}]_4[Pb_2Br_{11}]Br{\cdot}4H_2O$, it is obvious that water molecules replaced the DMSO solvent molecule and the 1D lead halide chains eventually cleaved into separated dimers. The overall reaction formula is as follows ($[C_4N_2H_{12}]$ is simplified as L)

$$4L_3[PbBr_5]_2{\cdot}4DMSO + 12H_2O \rightarrow 3L_4[Pb_2Br_{11}]Br{\cdot}4H_2O + 2PbBr_2 + 16\ DMSO$$

Not surprisingly, the 1D $[C_4N_2H_{12}]_3[PbBr_5]_2{\cdot}4DMSO$ is not stable under moisture, considering the weak interaction between the neutral DMSO molecule and other charged species. Thermal gravimetric analysis (TGA) of $[C_4N_2H_{12}]_3[PbBr_5]_2{\cdot}4DMSO$ shows a low degradation temperature at around 100 °C, which is attributed to the loss of the weakly bounded DMSO molecules (Figure S9). The intercalation of water also results in more N−H···O hydrogen bonds formed between cations and guest water molecules, which should lower the overall enthalpy of the crystal and favor the formation of a low-dimensional structure, as illustrated by Cui *et al.*[32] These results indicate that to develop highly stable low-dimensional perovskites, neutral solvent molecules should not exist in the crystal structure and organic cations with strongly hydrophilic groups should be avoided.

The structural change from 1D to 0D significantly alters the photophysical properties of the material. As shown in Figure 3b, the UV−vis absorption spectrum of 0D $[C_4N_2H_{12}]_4[Pb_2Br_{11}]Br{\cdot}4H_2O$ exhibits a single peak at 300 nm, which corresponds to its excitation peak of around 300 nm probed at 400 nm. The optical band gap was calculated to be 3.1 eV, which is larger than that of the 1D material. Interestingly, $[C_4N_2H_{12}]_4[Pb_2Br_{11}]Br{\cdot}4H_2O$ shows a deep-violet PL emission peaked at 392 nm when excited by 300 nm UV light. This is the first time that a high-energy PL emission extended to the UV range from low-dimensional organic−metal halide hybrid is observed. However, the PLQE of $[C_4N_2H_{12}]_4[Pb_2Br_{11}]Br{\cdot}4H_2O$ dramatically drops to 2.76%, hindering its real application as a light emitter. The lifetime of the 400 nm emission was determined to be 3.7 ns at room temperature and 55.5 μs at 77 K (Figure S10). The fast PL decay and the low PLQE suggests a much faster nonradiative than radiative decay pathway that dominates exciton recombination. The photophysical properties of $[C_4N_2H_{12}]Br$ and $PbBr_2$ are characterized, neither showing any PL peak at around 392 nm. We therefore consider the PL emission originating from the distorted excited states of the lead bromide dimer, same as that of previously reported 0D organic−metal halide clusters.[33,34] To confirm the PL mechanism, DFT calculation was also carried out for the 0D $[C_4N_2H_{12}]_4[Pb_2Br_{11}]Br{\cdot}4H_2O$. The nondispersive frontier band structure and the larger calculated band gap of 2.849 eV (Figure S11a) suggest the negligible electronic coupling of neighboring lead halide dimers. The projected DOS and spatial contours of the frontier orbitals (Figure S11b,c) further confirm that the excitation process mainly involves the transition from Pb 5s to Pb 5p on the lead halide dimers, validating that the emission comes from the excited dimer species.

We further fabricated a UV-pumped LED device by coating a UV chip (370 nm) with the mixture of polymethyl methacrylate (PMMA) and the powder of our 1D material to demonstrate its application as a down-converting phosphor. The assembled LED presented a reasonable white-light luminescence with a CRI of 78, a CCT of 4897 K, and a CIE coordinate of (0.3554, 0.4227) (Figure 4). Also, we continuously lit this encapsulated LED for over 24 h under ambient conditions and obtained relatively stable emission spectra (Figure S13). This result again proves the potential of $[C_4N_2H_{12}]_3[PbBr_5]_2{\cdot}4DMSO$ as a solid-state lighting material and confirms that the degradation of our 1D material is caused by moisture.

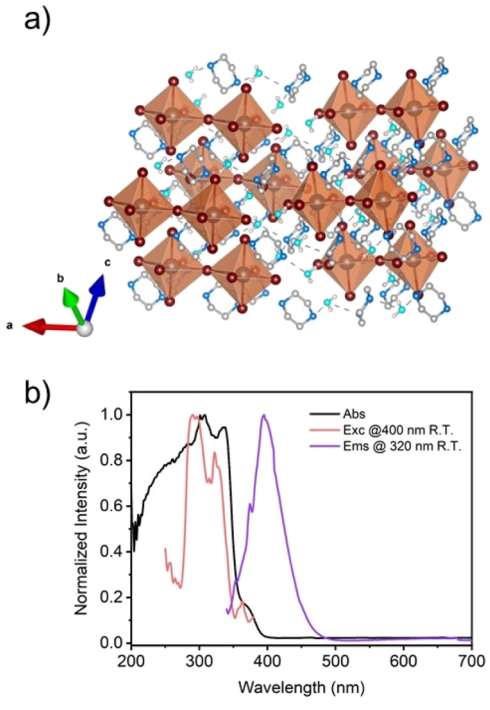

Figure 3. (a) Crystal structure of 0D $[C_4N_2H_{12}]_4[Pb_2Br_{11}]Br{\cdot}4H_2O$, in which corner-shared metal halide octahedron chains have broken into dimers. (b) Optical properties (absorption, excitation, and emission spectra) of $[C_4N_2H_{12}]_4[Pb_2Br_{11}]Br{\cdot}4H_2O$ crystals.

https://doi.org/10.1021/acs.chemmater.1c01219
Chem. Mater. 2021, 33, 5668−5674

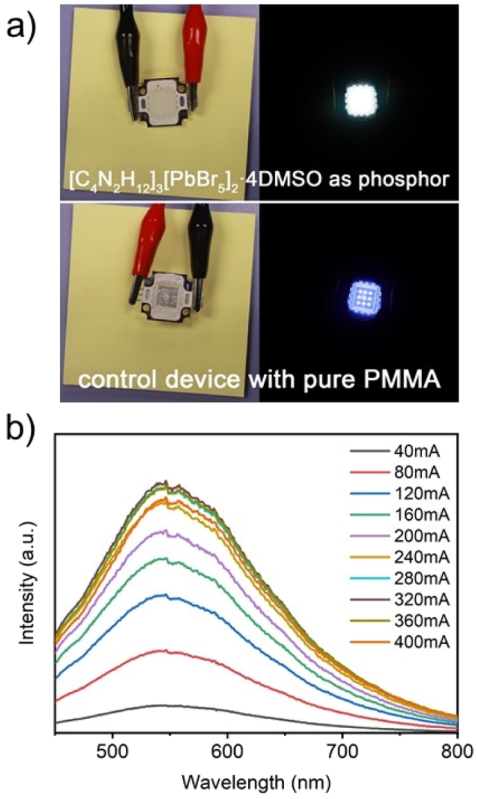

Figure 4. (a) Photographs of the LED device with or without $[C_4N_2H_{12}]_3[PbBr_5]_2$·4DMSO as phosphor. (b) Current dependent PL spectra of this LED device.

SUMMARY

In summary, we have developed a novel molecular 1D organic–metal halide hybrid, namely, $[C_4N_2H_{12}]_3[PbBr_5]_2$·4DMSO, in which the lead halide $[PbBr_5]_\infty$ 1D chains, $[C_4N_2H_{12}]^{2+}$ organic cations, and DMSO molecules are assembled into single crystals. This material exhibits a warm white-light emission with an outstanding PLQE of 60% and a CRI of 84, values among the best of those of 1D organic–metal halide hybrids reported to date. We also observed and studied its transformation from 1D to 0D under moisture conditions. The transformed product $[C_4N_2H_{12}]_4[Pb_2Br_{11}]Br·4H_2O$ is the first reported 0D organic–lead halide with unprecedent deep violet PL emission. With the experimental and calculated results, we conclude that the PL emissions of 1D $[C_4N_2H_{12}]_3[PbBr_5]_2$·4DMSO and 0D $[C_4N_2H_{12}]_4[Pb_2Br_{11}]Br·4H_2O$ originate from the self-trapped excitons and the distorted excited dimers, respectively. Our work suggests that a crystal structure with less hydrophilic groups and strong interaction between the components is essential to achieve highly stable organic–metal halide hybrid materials. With encapsulation, this 1D material could potentially replace current phosphors to achieve single-component white-light LEDs with UV LED as an optical pump source. It could also serve as an optical moisture sensor for various applications.

ASSOCIATED CONTENT

Supporting Information

The Supporting Information is available free of charge at https://pubs.acs.org/doi/10.1021/acs.chemmater.1c01219.

Experimental procedures, powder XRD, single-crystal structure, TGA, PL decay curves and exponential fitting, UV–vis spectra, PLQE, temperature-dependent emission spectra, and single-crystal data of $[C_4N_2H_{12}]_3[PbBr_5]_2$·4DMSO and $[C_4N_2H_{12}]_4[Pb_2Br_{11}]Br·4H_2O$; time lapse digital photographs, excitation-dependent spectra of $[C_4N_2H_{12}]_3[PbBr_5]_2$·4DMSO; calculated band structure, density of states, and the spatial contour plots of antibonding and bonding frontier orbitals of $[C_4N_2H_{12}]_4[Pb_2Br_{11}]Br·4H_2O$ (PDF)

AUTHOR INFORMATION

Corresponding Author

Haoran Lin − *Hoffmann Institute of Advanced Materials, Shenzhen Polytechnic, Shenzhen 518000, China;* orcid.org/0000-0003-0625-8881; Email: hlin@szpt.edu.cn

Authors

Guicheng Yu − *Hoffmann Institute of Advanced Materials, Shenzhen Polytechnic, Shenzhen 518000, China*

Fang Lin − *Hoffmann Institute of Advanced Materials, Shenzhen Polytechnic, Shenzhen 518000, China*

Kang Zhou − *Hoffmann Institute of Advanced Materials, Shenzhen Polytechnic, Shenzhen 518000, China*

Shaofan Fang − *International Collaborative Laboratory of 2D Materials for Optoelectronics Science and Technology of Ministry of Education, Institute of Microscale Optoelectronics, Shenzhen University, Shenzhen 518060, China*

Yumeng Shi − *International Collaborative Laboratory of 2D Materials for Optoelectronics Science and Technology of Ministry of Education, Institute of Microscale Optoelectronics, Shenzhen University, Shenzhen 518060, China;* orcid.org/0000-0002-9623-3778

Wei Liu − *School of Chemical Engineering and Technology, Sun Yat-Sen University, Zhuhai 519082, China*

Hanlin Hu − *Hoffmann Institute of Advanced Materials, Shenzhen Polytechnic, Shenzhen 518000, China*

Biwu Ma − *Department of Chemistry & Biochemistry, Florida State University, Tallahassee, Florida 32310, United States;* orcid.org/0000-0003-1573-8019

Complete contact information is available at: https://pubs.acs.org/10.1021/acs.chemmater.1c01219

Author Contributions

G.Y. completed most part of experiments and manuscript; F.L. conducted some part of the experiments; K.Z. determined the single-crystal structures; S.F. and Y.S. characterized the PLQE of the materials; W.L., H.H., and B.M. provided support to the ideas and manuscript writing; H.L. provided the idea and supervised this project.

Funding

National Natural Science Foundation of China (201901166), Guangdong Natural Science Foundation (2019A1515010692).

Notes

The authors declare no competing financial interest.

ACKNOWLEDGMENTS

We thank the National Natural Science Foundation of China (201901166) and Guangdong Natural Science Foundation (2019A1515010692) for financial support.

ABBREVIATIONS

PLQE	photoluminescence quantum efficiency
CRI	color rendering index
1D	one-dimensional
LEDs	light-emitting diodes
3D	three-dimensional
PL	photoluminescence
0D	zero-dimensional
DCM	dichloromethane
DMF	dimethylformamide
DMSO	dimethylsulfoxide
SCXRD	single-crystal X-ray diffraction
PXRD	powder X-ray diffraction
UV	ultraviolet−visible
CIE	Commission Internationale de ÍEclairage
CCT	correlated color temperature
DFT	density functional theory
PPW	pseudopotential plane wave
HOMO	highest occupied molecular orbital
DOS	density of states
TGA	thermal gravimetric analysis.

REFERENCES

(1) Stranks, S. D.; Snaith, H. J. Metal-halide perovskites for photovoltaic and light-emitting devices. *Nat. Nanotechnol.* **2015**, *10*, 391−402.

(2) Kakavelakis, G.; Gedda, M.; Panagiotopoulos, A.; Kymakis, E.; Anthopoulos, T. D.; Petridis, K. Metal Halide Perovskites for High-Energy Radiation Detection. *Adv. Sci.* **2020**, *7*, 2002098.

(3) Liu, X.-K.; Xu, W.; Bai, S.; Jin, Y.; Wang, J.; Friend, R. H.; Gao, F. Metal halide perovskites for light-emitting diodes. *Nat. Mater.* **2021**, *20*, 10−21.

(4) Hu, J.; Yan, L.; You, W. Two-Dimensional Organic-Inorganic Hybrid Perovskites: A New Platform for Optoelectronic Applications. *Adv. Mater.* **2018**, *30*, No. e1802041.

(5) Zhou, C.; Lin, H.; He, Q.; Xu, L.; Worku, M.; Chaaban, M.; Lee, S.; Shi, X.; Du, M.-H.; Ma, B. Low dimensional metal halide perovskites and hybrids. *Mater. Sci. Eng. R Rep* **2019**, *137*, 38−65.

(6) Wang, G.-E.; Sun, C.; Wang, M.-S.; Guo, G.-C. Semiconducting crystalline inorganic-organic hybrid metal halide nanochains. *Nanoscale* **2020**, *12*, 4771−4789.

(7) Yuan, Z.; Zhou, C.; Tian, Y.; Shu, Y.; Messier, J.; Wang, J. C.; van de Burgt, L. J.; Kountouriotis, K.; Xin, Y.; Holt, E.; Schanze, K.; Clark, R.; Siegrist, T.; Ma, B. One-dimensional organic lead halide perovskites with efficient bluish white-light emission. *Nat. Commun.* **2017**, *8*, 14051.

(8) Biswas, A.; Bakthavatsalam, R.; Shaikh, S. R.; Shinde, A.; Lohar, A.; Jena, S.; Gonnade, R. G.; Kundu, J. Efficient Broad-Band Emission from Contorted Purely Corner-Shared One Dimensional (1D) Organic Lead Halide Perovskite. *Chem. Mater.* **2019**, *31*, 2253−2257.

(9) Gautier, R.; Massuyeau, F.; Galnon, G.; Paris, M. Lead Halide Post-Perovskite-Type Chains for High-Efficiency White-Light Emission. *Adv. Mater.* **2019**, *31*, No. e1807383.

(10) Peng, Y.; Yao, Y.; Li, L.; Liu, X.; Zhang, X.; Wu, Z.; Wang, S.; Ji, C.; Zhang, W.; Luo, J. Exploration of Chiral Organic-Inorganic Hybrid Semiconducting Lead Halides. *Chem.−Asian J.* **2019**, *14*, 2273−2277.

(11) Liu, T.; Tang, W.; Luong, S.; Fenwick, O. High charge carrier mobility in solution processed one-dimensional lead halide perovskite single crystals and their application as photodetectors. *Nanoscale* **2020**, *12*, 9688−9695.

(12) Sun, C.; Guo, Y.-H.; Yuan, Y.; Chu, W.-X.; He, W.-L.; Che, H.-X.; Jing, Z.-H.; Yue, C.-Y.; Lei, X.-W. Broadband White-Light Emission in One-Dimensional Organic-Inorganic Hybrid Silver Halide. *Inorg. Chem.* **2020**, *59*, 4311−4319.

(13) Song, G.; Li, M.; Yang, Y.; Liang, F.; Huang, Q.; Liu, X.; Gong, P.; Xia, Z.; Lin, Z. Lead-Free Tin(IV)-Based Organic-Inorganic Metal Halide Hybrids with Excellent Stability and Blue-Broadband Emission. *J. Phys. Chem. Lett.* **2020**, *11*, 1808−1813.

(14) Yuan, H.; Massuyeau, F.; Gautier, N.; Kama, A. B.; Faulques, E.; Chen, F.; Shen, Q.; Zhang, L.; Paris, M.; Gautier, R. Doped Lead Halide White Phosphors for Very High Efficiency and Ultra-High Color Rendering. *Angew. Chem., Int. Ed.* **2020**, *59*, 2802−2807.

(15) Qi, Z.; Chen, Y.; Guo, Y.; Yang, X.; Zhang, F.-Q.; Zhou, G.; Zhang, X.-M. Broadband white-light emission in a one-dimensional organic−inorganic hybrid cadmium chloride with face-sharing CdCl6 octahedral chains. *J. Mater. Chem. C* **2021**, *9*, 88−94.

(16) Wu, S.; Zhou, B.; Yan, D. Low-Dimensional Organic Metal Halide Hybrids with Excitation-Dependent Optical Waveguides from Visible to Near-Infrared Emission. *ACS Appl. Mater. Interfaces* **2021**, *13*, 26451−26460.

(17) Sun, X.-Y.; Yue, M.; Jiang, Y.-X.; Zhao, C.-H.; Liao, Y.-Y.; Lei, X.-W.; Yue, C.-Y. Combining Dual-Light Emissions to Achieve Efficient Broadband Yellowish-Green Luminescence in One-Dimensional Hybrid Lead Halides. *Inorg. Chem.* **2021**, *60*, 1491−1498.

(18) Tan, L.; Luo, Z.; Chang, X.; Wei, Y.; Tang, M.; Chen, W.; Li, Q.; Shen, P.; Quan, Z. Structure and Photoluminescence Transformation in Hybrid Manganese(II) Chlorides. *Inorg. Chem.* **2021**, *60*, 6600−6606.

(19) Wang, Y.; Guo, S.; Luo, H.; Zhou, C.; Lin, H.; Ma, X.; Hu, Q.; Du, M.-h.; Ma, B.; Yang, W.; Lu, X. Reaching 90% Photoluminescence Quantum Yield in One-Dimensional Metal Halide C4N2H14PbBr4 by Pressure-Suppressed Nonradiative Loss. *J. Am. Chem. Soc.* **2020**, *142*, 16001−16006.

(20) Guo, S.; Zhao, Y.; Bu, K.; Fu, Y.; Luo, H.; Chen, M.; Hautzinger, M. P.; Wang, Y.; Jin, S.; Yang, W.; Lü, X. Pressure-Suppressed Carrier Trapping Leads to Enhanced Emission in Two-Dimensional Perovskite (HA)2 (GA)Pb2 I7. *Angew. Chem., Int. Ed.* **2020**, *59*, 17533−17539.

(21) Guo, S.; Bu, K.; Li, J.; Hu, Q.; Luo, H.; He, Y.; Wu, Y.; Zhang, D.; Zhao, Y.; Yang, W.; Kanatzidis, M. G.; Lü, X. Enhanced Photocurrent of All-Inorganic Two-Dimensional Perovskite Cs2PbI2Cl2 via Pressure-Regulated Excitonic Features. *J. Am. Chem. Soc.* **2021**, *143*, 2545−2551.

(22) Zhou, C.; Tian, Y.; Wang, M.; Rose, A.; Besara, T.; Doyle, N. K.; Yuan, Z.; Wang, J. C.; Clark, R.; Hu, Y.; Siegrist, T.; Lin, S.; Ma, B. Low-Dimensional Organic Tin Bromide Perovskites and Their Photoinduced Structural Transformation. *Angew. Chem., Int. Ed.* **2017**, *56*, 9018−9022.

(23) Gautier, R.; Paris, M.; Massuyeau, F. Hydrogen Bonding and Broad-Band Emission in Hybrid Zinc Halide Phosphors. *Inorg. Chem.* **2020**, *59*, 2626−2630.

(24) Robinson, K.; Gibbs, G. V.; Ribbe, P. H. Quadratic elongation: a quantitative measure of distortion in coordination polyhedra. *Science* **1971**, *172*, 567−570.

(25) Lü, X.; Stoumpos, C.; Hu, Q.; Ma, X.; Zhang, D.; Guo, S.; Hoffman, J.; Bu, K.; Guo, X.; Wang, Y.; Ji, C.; Chen, H.; Xu, H.; Jia, Q.; Yang, W.; Kanatzidis, M. G.; Mao, H.-K. Regulating off-centering distortion maximizes photoluminescence in halide perovskites. *Natl. Sci. Rev.* **2020**, *0*, nwaa288.

(26) Navrotsky, A. Pressure-induced structural changes cause large enhancement of photoluminescence in halide perovskites: a quantitative relationship. *Natl. Sci. Rev.* **2021**, *0*, nwab041.

(27) Wu, G.; Zhou, C.; Ming, W.; Han, D.; Chen, S.; Yang, D.; Besara, T.; Neu, J.; Siegrist, T.; Du, M.-H.; Ma, B.; Dong, A. A One-Dimensional Organic Lead Chloride Hybrid with Excitation-Dependent Broadband Emissions. *ACS Energy Lett.* **2018**, *3*, 1443−1449.

(28) Smith, M. D.; Connor, B. A.; Karunadasa, H. I. Tuning the Luminescence of Layered Halide Perovskites. *Chem. Rev.* **2019**, *119*, 3104−3139.

(29) Manser, J. S.; Christians, J. A.; Kamat, P. V. Intriguing Optoelectronic Properties of Metal Halide Perovskites. *Chem. Rev.* **2016**, *116*, 12956−13008.

https://doi.org/10.1021/acs.chemmater.1c01219
Chem. Mater. 2021, 33, 5668−5674

(30) Fluorophores. In *Principles of Fluorescence Spectroscopy*; Lakowicz, J. R., Ed.; Springer US: Boston, MA, 2006; Chapter 3, pp 63−95.
(31) Manser, J. S.; Saidaminov, M. I.; Christians, J. A.; Bakr, O. M.; Kamat, P. V. Making and Breaking of Lead Halide Perovskites. *Acc. Chem. Res.* **2016**, *49*, 330−338.
(32) Cui, B.-B.; Han, Y.; Huang, B.; Zhao, Y.; Wu, X.; Liu, L.; Cao, G.; Du, Q.; Liu, N.; Zou, W.; Sun, M.; Wang, L.; Liu, X.; Wang, J.; Zhou, H.; Chen, Q. Locally collective hydrogen bonding isolates lead octahedra for white emission improvement. *Nat. Commun.* **2019**, *10*, 5190.
(33) Zhou, C.; Lin, H.; Tian, Y.; Yuan, Z.; Clark, R.; Chen, B.; van de Burgt, L. J.; Wang, J. C.; Zhou, Y.; Hanson, K.; Meisner, Q. J.; Neu, J.; Besara, T.; Siegrist, T.; Lambers, E.; Djurovich, P.; Ma, B. Luminescent zero-dimensional organic metal halide hybrids with near-unity quantum efficiency. *Chem. Sci.* **2018**, *9*, 586−593.
(34) Zhou, J.; Li, M.; Ning, L.; Zhang, R.; Molokeev, M. S.; Zhao, J.; Yang, S.; Han, K.; Xia, Z. Broad-Band Emission in a Zero-Dimensional Hybrid Organic [PbBr6] Trimer with Intrinsic Vacancies. *J. Phys. Chem. Lett.* **2019**, *10*, 1337−1341.

https://doi.org/10.1021/acs.chemmater.1c01219
Chem. Mater. 2021, 33, 5668−5674